Supplemental material

Tripathi et al., https://doi.org/10.1083/jcb.201810098

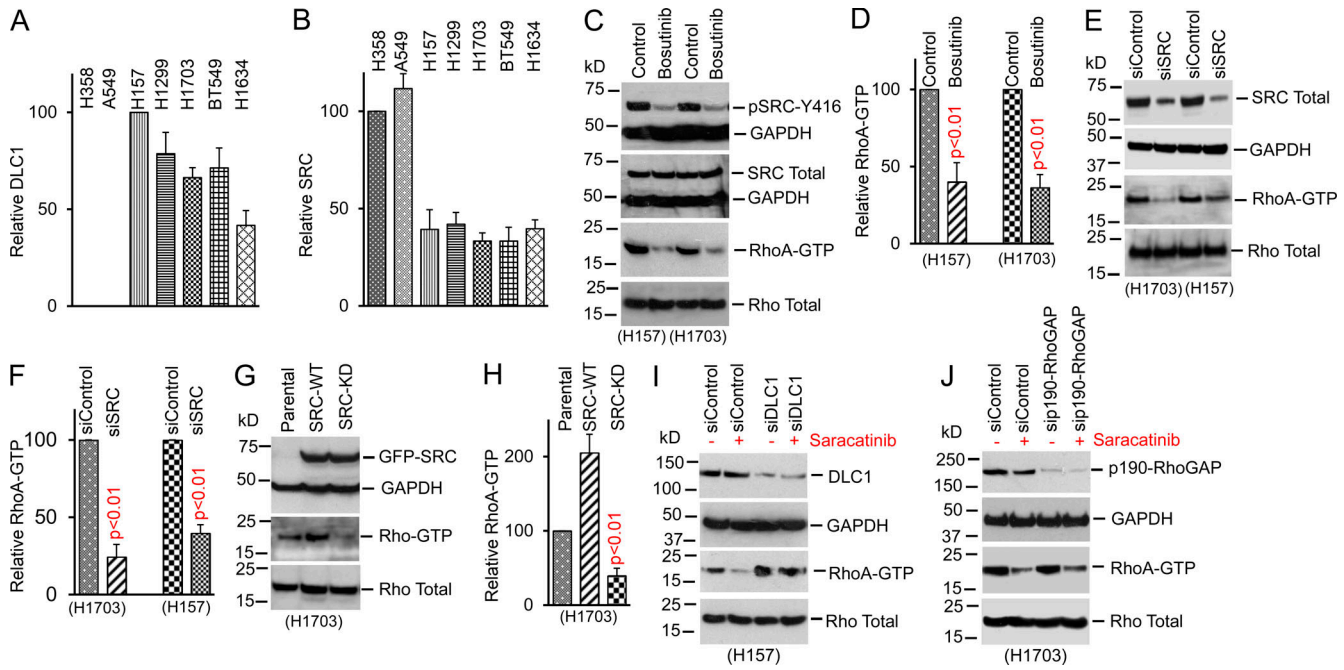

Figure S1. **SRC activity increases RhoA-GTP through DLC1. (A and B)** There is an inverse relationship between the level of DLC1 protein and the level of SRC protein. Graph in A shows relative levels DLC1 protein ± SD from three experiments, and graph in B shows relative levels of SRC protein ± SD from three experiments. Representative IBs for these data are shown in Fig. 1 A. **(C)** IB showing that bosutinib inhibited SRC activity (top) and decreased RhoA-GTP (lower middle) in DLC1-positive H157 and H1703 cancer lines but did not alter total SRC (upper middle) or total Rho (bottom). GAPDH was used as a loading control. **(D)** Graph shows relative RhoA-GTP ± SD from three experiments, as shown in C. Parametric two-tailed *t* tests were performed for all statistical analyses. **(E)** SRC siRNAs decreased SRC protein in H1703 and H157 lines (top) and decreased RhoA-GTP. Experimental conditions and data display were as in C, except cells were treated with SRC siRNAs. **(F)** Graph shows relative RhoA-GTP ± SD from three experiments, as shown in E. **(G)** SRC-WT substantially increased RhoA-GTP, but not total Rho, in a DLC1-positive H1703 line. Kinase-dead SRC reduced RhoA-GTP, but not total Rho. **(H)** Graph shows relative RhoA-GTP ± SD from three experiments, as shown in G. **(I)** Saracatinib decreased RhoA-GTP in parental H157 cells, but not in DLC1-knockdown cells. **(J)** Saracatinib decreased RhoA-GTP in both p190–Rho-GAP–expressed and p190–Rho-GAP–knockdown H1703 cells.

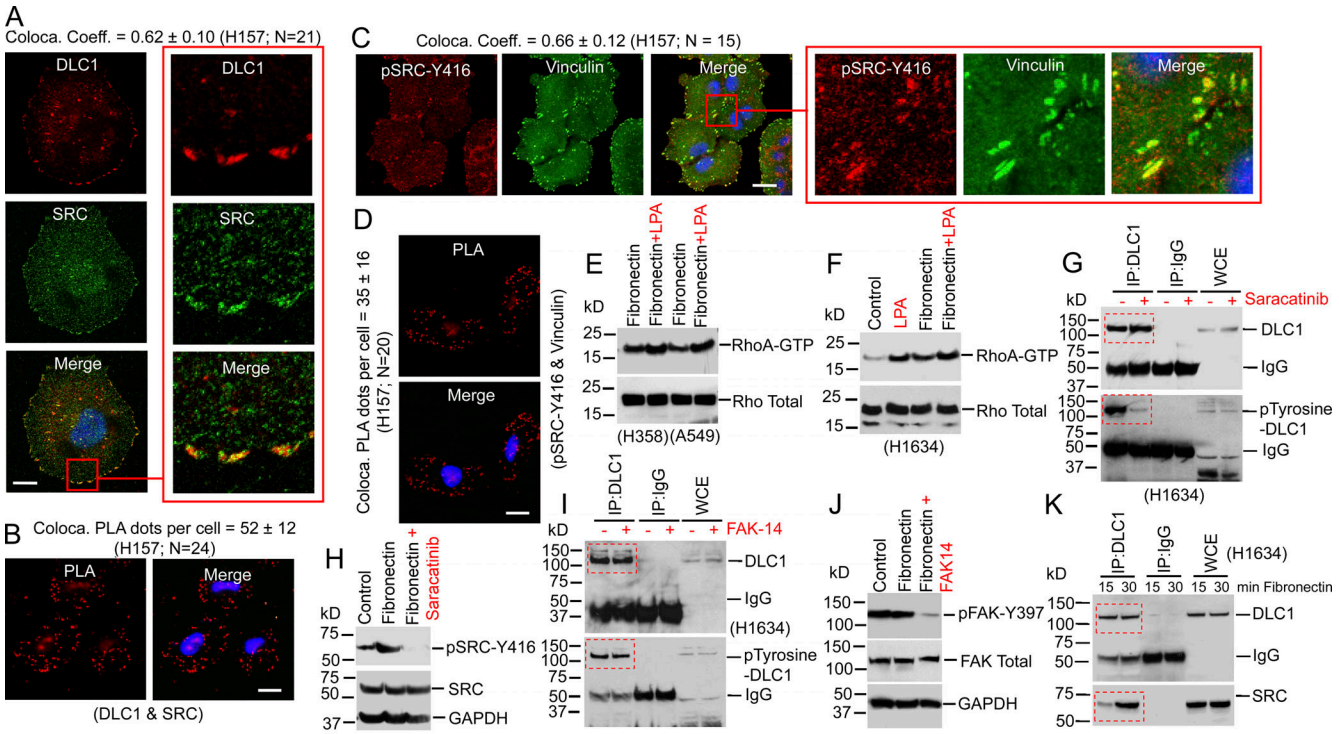

Figure S2. **SRC colocalizes with DLC1, and LPA increases RhoA-GTP independently of DLC1. (A)** Colocalization of SRC with DLC1. H157 cells were immunostained with DLC1 (red) and SRC (green) antibodies. Colocalization of DLC1 and SRC is highlighted in red box. Red box in the merge image is a zoomed in view of the selected area that highlights the colocalization between DLC1 (red) and SRC (green). Averaged overlapping colocalization coefficient ± SD was calculated from 21 cells randomly selected from several fields. Scale bar, 20 µm. **(B)**. Colocalization of DLC1 and SRC was confirmed by PLA. Scale bar, 20 µm. **(C)** Colocalization of kinase-active SRC (pSRC-Y416) with vinculin. H157 cells were stained with pSRC-Y416 (red) and vinculin (green) antibodies. Colocalization of pSRC-Y416 (red) and vinculin is highlighted in red box. Red box in the merge image is a zoomed in view of the selected area that highlight the colocalization between pSRC-Y416 (red) and vinculin (green). Averaged overlapping colocalization coefficient ± SD was calculated from 15 cells randomly selected from several fields. Scale bar, 20 µm. **(D)** Colocalization of pSRC-Y416 and vinculin was confirmed by PLA. Scale bar, 20 µm. **(E)** LPA increases RhoA-GTP in DLC1-negative lines. Combined treatment of LPA and fibronectin induces higher RhoA-GTP than fibronectin alone in DLC1-negative H358 and A549 lines. **(F)** LPA increased RhoA-GTP comparable to fibronectin treatment; however, the combined treatment of LPA and fibronectin has higher RhoA-GTP than their individual treatment. LPA and fibronectin did not alter total Rho (bottom). **(G)** Saracatinib reduces tyrosine phosphorylation of DLC1 induced by fibronectin. Non-transformed H1634 cells were plated on fibronectin and treated without or with saracatinib. Lysates from treated cells were IP with DLC1 or mock IgG antibodies followed by IB with DLC1 (top) or pTyrosine (bottom) antibodies. **(H)** Fibronectin treatment increased SRC kinase activity, and saracatinib treatment reduced the SRC activity, as determined by pSRC-Y416. Fibronectin and saracatinib did not alter total SRC protein. GAPDH was used as a loading control. **(I)** FAK inhibitor FAK-14 did not alter DLC1 tyrosine phosphorylation induced by fibronectin (highlighted in red-dotted rectangle). H1634 cells were plated on fibronectin and treated without or with FAK-14. Lysates from treated cells were IP with DLC1 or mock IgG antibodies, followed by IB with DLC1 (top) or pTyrosine (bottom) antibodies. **(J)** Fibronectin did not alter the FAK activity, as determined by pFAK-Y397. However, FAK inhibitor FAK-14 reduced the FAK activity. Fibronectin and FAK-14 did not alter total FAK protein level. GAPDH was used as a loading control. **(K)** Fibronectin induced increased complex formation between DLC1 and SRC at 30 min. H1634 cells were plated on fibronectin for 15 and 30 min. Lysates were IP with DLC1 or mock IgG antibodies followed by IB with DLC1 (top) or SRC (bottom) antibodies.

A

Phosphorylation of DLC1-Y451 and DLC1-Y701 were SRC kinase dependent

Phosphorylated Peptide Sequence	Modifications	Phosphorylated / Total Peptides	XCorr	Charge
Flag-Control				
LSIYDNVPGSIL**Y(ph)**SSSGDLADLENEDIFPELDDILYHVK **(Y451)**	Y13(Phospho)	7/20	6.30	4
QMNEGAIDCVN**Y(ph)**EGQSAYDVADMLK **(Y701)**	M2(Oxidation) C9(Carbamidomethyl) Y12(Phospho)	3/14	7.03	3
Flag-SRC-Kinase-Active				
LSIYDNVPGSIL**Y(ph)**SSSGDLADLENEDIFPELDDILYHVK **(Y451)**	Y13(Phospho)	21/23	6.04	4
QMNEGAIDCVN**Y(ph)**EGQSAYDVADMLK **(Y701)**	M2(Oxidation) Y12(Phospho) M23(Oxidation)	25/27	4.0	3
Flag-SRC-Kinase-Dead				
LSIYDNVPGSIL**Y**SSSGDLADLENEDIFPELDDILYHVK (Y451)		0/16	4.27	4
QMNEGAIDCVN**Y**EGQSAYDVADMLK (Y701)	M2(Oxidation) C9(Carbamidomethyl)	0/26	7.27	3

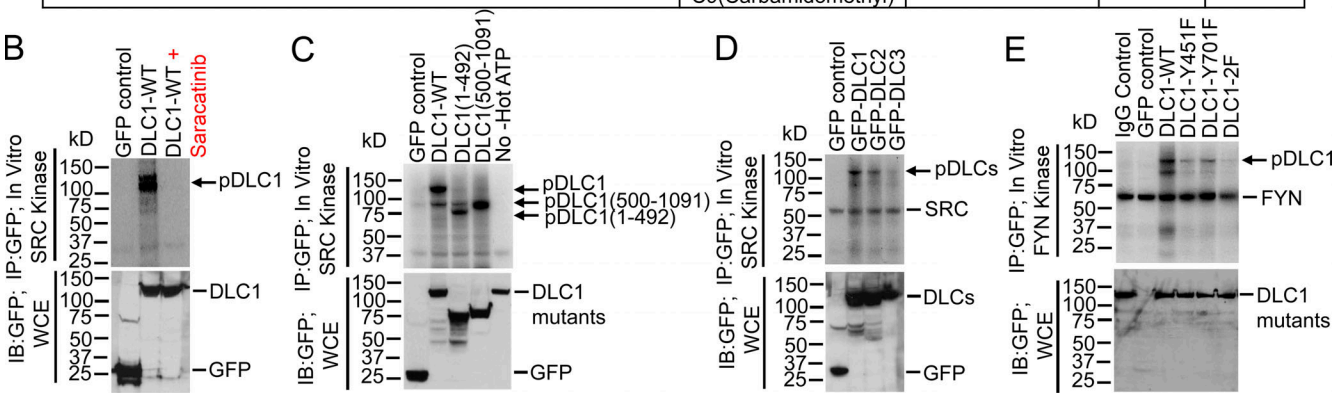

Figure S3. **DLC1, DLC2, and DLC3 are SRC substrates. (A)** Phosphorylation of DLC1-Y451 and DLC1-Y701 by SRC in vivo. DLC1 phosphopeptides were detected by mass spectrometry. The phosphorylation signals were fully localized to the indicated tyrosines in phosphopeptides in the presence of kinase-active SRC, but were absent in the presence of kinase-dead SRC. Xcorr is a statistical cross-correlation factor that defines the quality of MS2 spectra. **(B)** SRC phosphorylates DLC1 in vitro. Top: IP DLC1-WT from transfected HEK 293T cells was strongly phosphorylated in vitro by recombinant SRC kinase (lane 2), as detected with ^{32}P autoradiography; GFP control was negative (lane 1). Saracatinib decreased the phosphorylation signal produced by SRC kinase. Bottom: Expression of GFP and DLC1 constructs is shown. **(C)** SRC phosphorylates N-terminal and C-terminal DLC1 fragments in vitro. Top: IP DLC1-WT was strongly phosphorylated in vitro by recombinant SRC kinase (lane 2), as detected with ^{32}P autoradiography. GFP control gave no phosphorylation signal (lane 1). Both the DLC1 N-terminal and C-terminal fragments were phosphorylated (lanes 3 and 4). Bottom: Expression of GFP and GFP-tagged DLC1 constructs. **(D)** Other members of DLC family, DLC2 and DLC3, were also phosphorylated by SRC kinase, but less strongly than DLC1. **(E)** FYN phosphorylates DLC1 in vitro. Top: IP DLC1-WT from transfected HEK 293T cells was phosphorylated in vitro by recombinant FYN kinase (lane 3), as detected with ^{32}P autoradiography. IgG control and GFP control were negative (lanes 1 and 2). Single mutants (DLC1-Y451F or DLC1-Y701F) were weakly phosphorylated (lanes 4 and 5), but the combined DLC1-2F mutant (DLC1-Y451F,Y701F) gave a barely detectible phosphorylation signal (lane 6). Bottom: Expression of DLC1 constructs is shown.

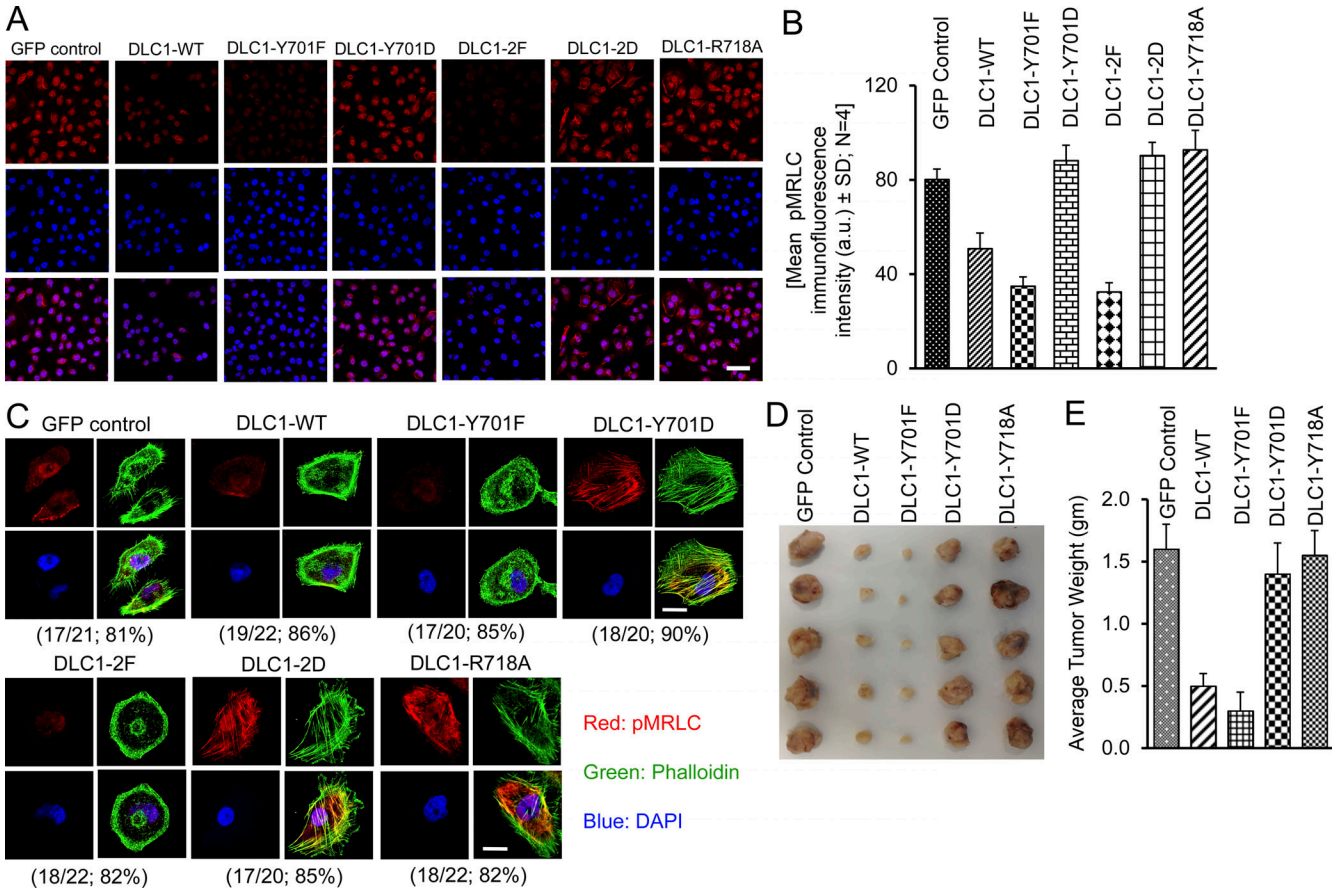

Figure S4. **RhoA-GTP and downstream targeting are regulated by SRC phosphorylation of DLC1. (A)** H1703 cells with stably transfected DLC1-WT, DLC1-Y701F, or DLC1-2F have less phospho-MRLC (red), a downstream RhoA target, compared with the other transfectants. DAPI (blue) represents nuclei. Scale bar, 100 µm. **(B)** Graph shows the relative pMRLC immunofluorescence intensity ± SD from four experiments, as shown in A. **(C)** H1703 cells stably transfected with DLC1-WT, DLC1-Y701F, or DLC1-2F have fewer concave boundaries, consistent with reduced contraction, and fewer stress fibers (green), especially in the central region, compared with the other transfectants. The confocal images are representative of a majority of the cells. Scale bars, 20 µm. **(D and E)** Xenograft tumors from mice excised 6 wk after injecting stable transfectants. **(D)** Photographs of excised tumors. **(E)** Graph shows average tumor weight (g) ± SD for each group. DLC1-Y701D is as defective for tumor suppression as GAP-dead DLC1-R718A.

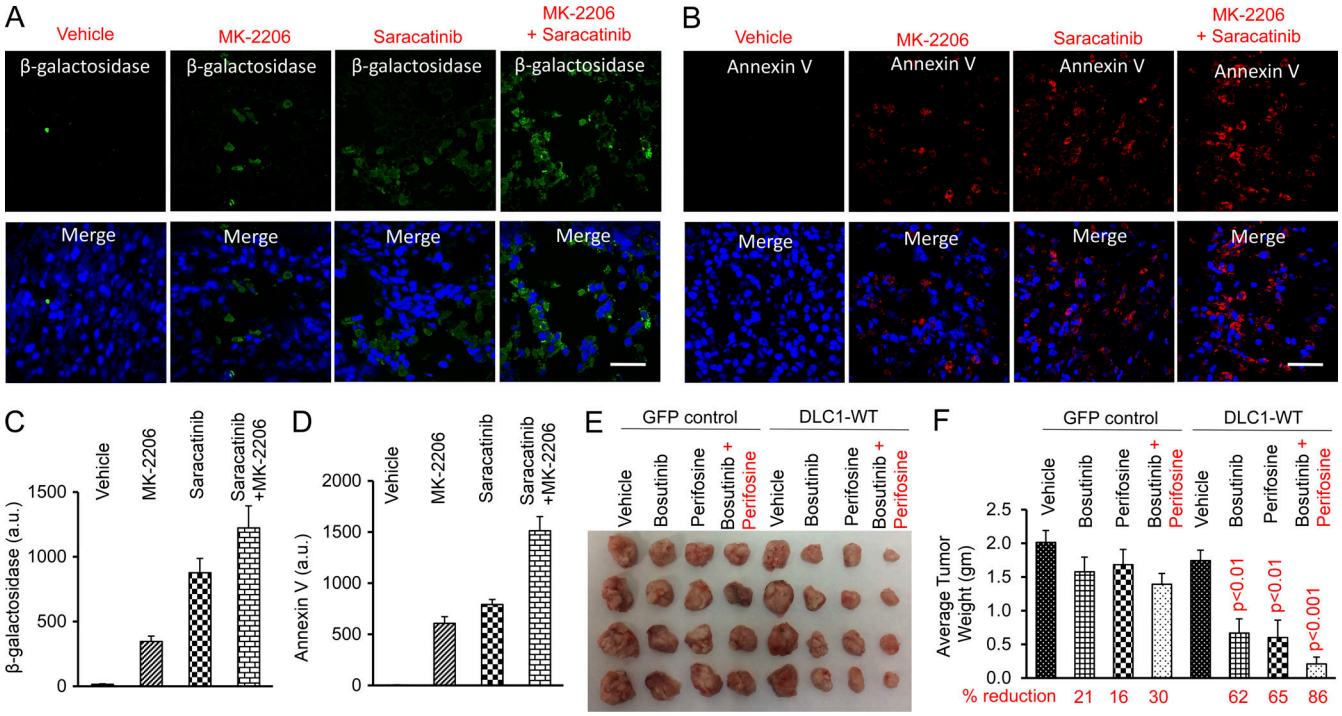

Figure S5. **Saracatinib and MK-2206 treatment induces cellular senescence and apoptosis in DLC1-WT tumors. (A–D)** In DLC1-WT tumors shown in Fig. 9 A, which were treated with saracatinib and/or MK-2206, saracatinib or MK-2206 alone induced cellular senescence (A), as measured by β-galactosidase, and apoptosis (B), as measured by annexin V. Scale bars, 50 µm. The combined treatment of saracatinib and MK-2206 leads to increased signals for both β-galactosidase and annexin V. Quantitation of the β-galactosidase signals ± SD is shown in C, and quantitation of the annexin V signals ± SD is shown in D. **(E and F)** After the H358 xenograft tumor size reached ~1.0 cm in diameter, mice with tumors were treated for 5 d with the SRC inhibitor bosutinib alone, with the AKT inhibitor perifosine alone, or with the two drugs in combination. **(E)** Photographs of excised tumors. **(F)** Graph shows average tumor weight (g) ± SD for each group. The percentage of reduced tumor weight from treatment with bosutinib and/or perifosine, compared with the vehicle control. In DLC1-WT tumors, combined treatment with bosutinib and perifosine suppressed tumor growth more strongly than the individual inhibitors.